Journal of Organometallic Chemistry 694 (2009) 3172–3178

Contents lists available at ScienceDirect

Journal of Organometallic Chemistry

journal homepage: www.elsevier.com/locate/jorganchem

Application of heteroleptic iridium complexes with fluorenyl-modified 1-phenylisoquinoline ligand for high-efficiency red polymer light-emitting devices

Bo Liang [a,b,*], Lei Wang [a], Xuhui Zhu [a], Huahong Shi [a], Junbiao Peng [a], Yong Cao [a,*]

[a] Institute of Polymer Optoelectronic Materials and Devices, South China University of Technology, Guangzhou 510640, PR China
[b] School of Automobile and Mechanic Engineering, Changsha University of Science and Technology, Changsha 410076, PR China

ARTICLE INFO

Article history:
Received 15 March 2009
Received in revised form 3 May 2009
Accepted 11 May 2009
Available online 18 May 2009

Keywords:
Iridium complexes
Phosphorescence
Polymer light-emitting devices

ABSTRACT

A series of new heteroleptic iridium complexes bearing fluorenyl-modified 1-phenylisoquinoline as the first ligand and different ancillary ligands has been prepared and characterized. These complexes bis(1-(3-(9,9-dimethyl-fluoren-2-yl)phenyl)isoquinoline-C2,N′)iridium(III)acetylacetonate(Ir(DMFPQ)$_2$acac)), bis(1-(3-(9,9-dimethyl-fluoren-2-yl)phenyl)isoquinoline-C2,N′)iridium(III)(3-(pyridin-2-yl)-1,2,4-triazolate)(Ir(DMFPQ)$_2$pt) and bis(1-(3-(9,9-dimethyl-fluoren-2-yl)phenyl)isoquinoline-C2,N′)iridium(III)(2-(2-pyridyl)benzimidazolate)(Ir(DMFPQ)$_2$pbi) showed red phosphorescent emissions of 615–630 nm in dichloromethane solution. The device fabricated with these complexes doped into a host polyfluorene (PFO) blend with 30% of an electron transport material 2-(4-biphenyl)-5-(4-*tert*-butylphenyl)-1,3,4-oxadiazole (PBD) showed high device efficiencies. Ir(DMFPQ)$_2$acac exhibited red emission with an external quantum efficiency(η_{ext}) of 14.3% and luminous efficiency(η_c) of 7.8 cd/A at 1.2 mA/cm^2 and the maximum brightness reached 10 006 cd/m^2 (Commission Internationale de l'Eclairage(CIE) chromaticity coordinates: (0.67, 0.32)) at 412 mA/cm^2. Ir(DMFPQ)$_2$pt showed a η_{ext} of 13.0% and η_c of 9.2 cd/A at 17 mA/cm^2, 1532 cd/m^2, and the maximum brightness reached 15085 cd/m^2 (CIE: 0.64, 0.34) at 360 mA/cm^2.

1. Introduction

Organic/polymer phosphorescent light-emitting diodes materials (O/PPhLEDs) have attracted great attention because of their potentially applications in flat panel displays [1]. Nearly 100% of internal quantum efficiency corresponding to the harvesting of all singlet and triplet states can be achieved in devices composed of phosphorescent complexes based on osmium (Os) [2,3], iridium (Ir) [4,5] and platinum (Pt) complexes [6]. Due to the relatively short triplet lifetime (1–14 μs), potential high device efficiency and emission wavelength tunability from blue to deep red, over the entire visible spectrum and high-efficiency, Ir(III)-based phosphorescent cyclometalated complexes are attracting much particular attention as the efficient dopant for applications in the area of O/PPhLEDs. Great progresses have been made in designing materials and optimizing device configuration, and high external and power device efficiencies have been obtained [7–9]. A green phosphorescent device with heteroleptic complex, Ir(ppy)$_2$acac, doped into a small molecular host has been reported showing a high η_{ext} of 19% and a power efficiency (η_p) of 60 lm/W (ppy = 2-phenylpyridine; acac = acetylacetone) [10]. In order to take advantage of solution processing such as spin-coating or ink-printing, which is suitable for making large area displays, PPhLEDs with a wide-band gap semiconducting blue-emitting polymer host have been widely investigated [11,12]. Gong et al. reported high-efficiency yellow to red-emitting PLEDs of η_{ext} = 5% ph/el and η_c = 7.2 cd/A with an emission maximum at 600 nm by doping Ir(HFP)$_3$ [tris(2,5-bis-2′-(9′,9′-dihexylfluorene) pyridine)iridium(III)] into PVK:PBD (40%) [PVK = poly(*N*-vinylcarbazole) [13]. Jiang et al. developed some red phosphorescent devices involving the use of polymer PFO:PBD (30%) as the host materials doped with bis(1-phenylisoquinoline)Ir(III)acetylactonate[PhqIr] as the guest, and obtained saturated red PPhLEDs with a η_{ext} up to 12% and a peak luminous efficiency 5.2 cd/A [14]. Polymer organic light-emitting devices based on a Ir-complex Ir(MPCPPZ)$_3$ (tris(1-(2,6-dimethylphenoxy)-4-(4-chlorophenyl)phthalazine)iridium(III)) exhibited the highest external quantum efficiency of 20.2% and luminance efficiency of 18.4 cd/A. The efficiency remains as high as 6.6% at a current density of 100 mA/cm^2 [8]. Among them, the heteroleptic cyclometalated iridium complexes show good device as homoleptic ones. These complexes have two cyclometalated ligands and an ancillary ligand. The emission color from the heteroleptic complexes is dependent on the choice of both the cyclometalated ligand and ancillary ligands. You et al. [15] recently reported color tuning over the whole visible range by changing the ancillary ligands. Ostrowski et al. designed a series of Ir complexes with fluorene-modified phenylpyridine ligand resistant to crystallization, and obtained green and orange emission [16]. Huang et al report saturated red organic light-emitting diodes with iridium com-

* Corresponding authors.
E-mail addresses: lbscut@yahoo.com.cn (B. Liang), poycao@scut.edu.cn (Y. Cao).

0022-328X/$ - see front matter © 2009 Elsevier B.V. All rights reserved.
doi:10.1016/j.jorganchem.2009.05.009

plexes bearing fluorene-modified polyphenylphenyl dendron ligands, the efficiencies reached to 42.5 cd/A and 12.8%, respectively [17]. It was reported that triazolyl pyridine ligand could be used to be ancillary ligands to prepare blue phosphorescent complexes [18,19] and benzoimidazoles as cyclometalated ligands to prepare high thermal stability green to yellow complexes [20,21].

However, the performance of PPhLEDs is still lower than that of small molecule-based host devices. For example, Tsuboyama et al. [22] reported $Ir(piq)_3$, a phosphorescent dopant, achieved a high external quantum efficiency, η_{ext} = 10.3% at 100 cd/m^2. Duan et al. [23] reported a device based on (2-methyldibenzo[f,h]quinoxalino(C2, N′)) Ir(III) acetylacetonate ($Ir(MDQ)_2acac$) with high η_{ext} of 12.4% with the device structure: NPB(50 nm)/$Ir(MDQ)_2$-acac:CBP(5.7%, 30 nm)/TPBI(15 nm)/Alq(35 nm). The iridium complexes containing the 1-phenylisoquinoline type of cyclometalated ligands, such as $Ir(piq)_2acac$, have been studied for the fabrication of saturated red O/PPhLEDs [24–26].

The purpose of the present study is the molecular designs of high-efficient red phosphorescent complexes with good charge-transporting properties. We designed and synthesized a new cyclometalated ligand: 1-(3-(9,9-dimethyl-fluoren-2-yl)phenyl)isoquinoline. Combination of this new ligand with acetylacetone provides PPhLEDs with a saturated red emission of excellent device efficiency (over 14%). Accepted traditional ancillary ligand, acetylacetone, 3-(pyridin-2′-yl)-2*H*-1,2,4-triazole and 2-(2-pyridyl)benzimidazole were compared as an ancillary ligand for red emitters. We found out that triazole or benzoimidazole ancillary ligands lead to a little blue shift (around 20 nm) but result in good device efficiency and more gentle decay in efficiency at high current density and as well as at high doping concentration. It is a report that the efficiency of the saturated red phosphorescent devices by spin-coating from the polymer host reached the level comparable with that of the small molecular light-emitting diodes based on vacuum deposition.

2. Results and discussions

2.1. Syntheses

A new 1-phenylisoquinoline derivative 1-(3-(9,9-dimethyl-fluoren-2-yl) phenyl)isoquinoline **7** as cyclometalated ligand is synthesized. The synthesis involved the successful preparation of a key intermediate 1-(3-bromophenyl)-3,4-dihydroisoquinoline **2** that allowed further delicate functionalizations. The substituent 9,9-dimethylfluorenyl of **7** is at a *meta* position with respect to the "1-phenyl" ring, possibly acting us a solubilizing and bulky group, reducing the photoluminescent quenching of the resultant Ir complexes in the solid state and improving compatibility with the polymer host. In the preparation of heteroleptic Ir complexes, acetylacetone (**acac**), 3-(pyridin-2-yl)-2*H*-1,2,4-triazole (**pt**) and 2-(2-pyridyl)benzimidazole (**pbi**) were chosen as ancillary ligands.

Reflux of a mixture of **7** and $IrCl_3{\cdot}3H_2O$ in 3:1(v/v) 2-methoxyethanol and H_2O yielded the chloro-bridged dimeric precursor **8**. Complex **9** was prepared through the reaction of dimer **8** with excess of acetylacetone in 2-ethoxyethanol in the refluxed condition according to the literature [23]. "Since the ancillary ligand (pt) and 2-(2-pyridyl)benzimidazole(pbi) possesses two possible coordinated N atoms, there may arise two different Ir complexes: charged complex with protonated triazole ligand and neutral complex with deproton. Under basic conditions, the target heteroleptic Ir complexes **10**, **11** were obtained facilely by reaction of **8** with pt and pbi in high yields. The triazole or benzimidazole site is readily to lose a proton from the NH fragment to form a stable anionic ligand, subsequently producing neutral chelate complexes. We deprotonated pt or pbi with sodium methoxide before mixing it with chloride-bridged Ir dimer in order to preferably obtain a pure isomer for Ir complexes **10**, **11**."

Table 1
Optical data of the isoquinoline ligand **7** and iridium complexes **9–11** in CH_2Cl_2 solution.

Compounds	Absorbance (nm)	Emission (nm)
7	228, 292, 316	
9	292, 337, 481	630
10	299, 334, 470	615
11	292, 328, 466	612

2.2. Optical and photoluminescent properties of Ir complexes

Table 1 lists the UV data of the complexes in dichloromethane solution. A band with the maximum absorbance at around 330 nm shows the same shape as that of the free ligand **7**, but with about 20 nm bathochromic shifts. This indicates that the intense absorption bands at the wavelength region are assigned to ligand-centered electronic transitions [27]. UV–Vis absorption spectra of the complexes **9**, **10**, **11** (neat film) and PL spectra of the host PFO–PBD (30%) (in film), complexes **9**, **10**, **11** (in CH_2Cl_2 solution) are shown in Fig. 1. All the complexes show broad absorption bands in the wavelength region of 450–600 nm. These weak bands located at a long wavelength have been assigned to the $S_0 \rightarrow {}^1$MLCT and $S_0 \rightarrow {}^3$MLCT transitions of iridium complexes [28]. In comparison with the absorption band of $Ir(1\text{-}piq)_2acac$, a marked bathochromic shift is observed for **9**, presumably owing to a large π conjugation system of ligand **7**. There is a good overlap between the emission spectra of host PFO–PBD (30%) and the absorption spectra of guests (Ir complexes, **9**, **10** and **11**), which meet the requirements of the efficient Förster transfer from the host polymer to the Ir complexes. The PL peak of the complexes with triazole and benzoimidazole derivatives as ancillary ligands has a blue shift compared with the complex with acetylacetone as ancil-

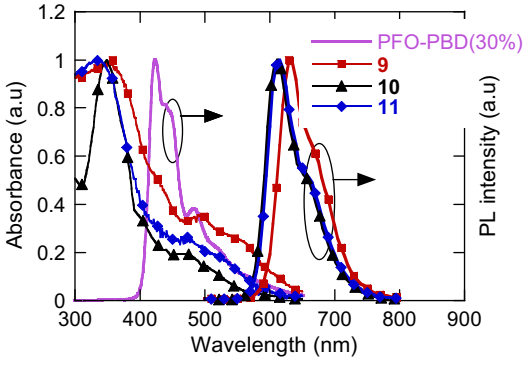

Fig. 1. UV–Vis absorption spectra of the complexes **9–11** (in the films), PL spectra of PFO–PBD (30 wt.%) (film) and the complexes **9–11** (in CH_2Cl_2).

Table 2
Electrochemical data of the isoquinoline ligand **7** and iridium complexes **9–11** in CH_2Cl_2 solution.

Compounds	E_{opt}[a]	E_{ox}^{onset}	HOMO	LUMO[b]
7	3.62	2.27	−6.67	−3.05
9	1.92	0.52, 1.22	−4.92	−3.00
10	2.09	0.57, 1.25	−4.97	−2.88
11	2.16	0.65, 1.24	−5.05	−2.89

[a] Estimated from the absorption onset.
[b] Calculated from the optical band gap E_{opt} and oxidation potential (onset).

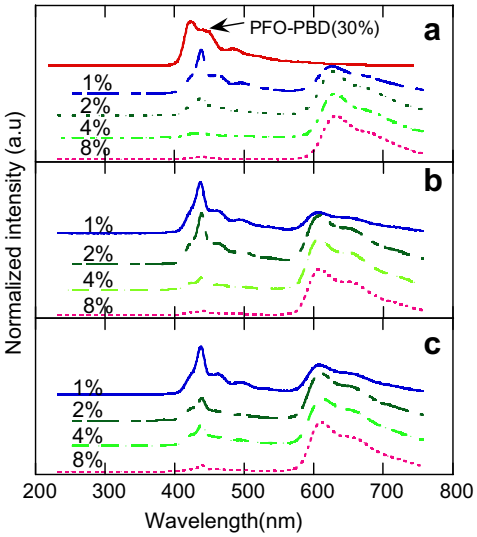

Fig. 2. PL spectra of PFO–PBD (30 wt.%) films and complexes-doped into PFO + PBD(30 wt.%) films in different doping concentrations, a (**9**), b (**10**), c (**11**).

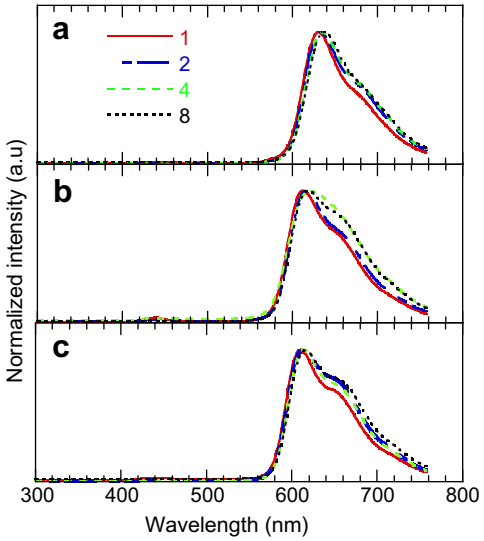

Fig. 3. EL spectra of complexes-doped PFO–PBD (30 wt.%) films in different doping concentrations, a (**9**), b (**10**), c (**11**).

lary ligand. The data were shown in Table 1. This is because of the different energy level of the different ancillary ligands [27].

2.3. Electrochemical analysis

The electrochemical properties of the Ir complexes were investigated by cyclic voltammetry (CV) with platinum as working electrode and saturated calomel electrode (SCE) as the reference electrode, with nitrogen-saturated dichloromethane solution of 0.1 M tetrabutylammonium hexafluorophosphate ($Bu_4N^+PF_6^-$). Table 2 lists the electrochemical data of cyclometalated ligand and complexes. The complexes show a quasi-reversible oxidation wave with onset voltages at around 0.6 V, which can be assigned to the oxidation process occurring mainly at the Ir metal center cationic site, together with a minor contribution from the cyclometalated phenyl fragment, which is consistent with the reported data [27,29]. We were unable to record the reversible reduction processes. HOMO levels of the compounds are calculated according to the empirical formulas $E_{HOMO} = -e(E_{ox} + 4.4)$(eV) [30]. The optical band gaps (E_{opt}) were estimated from the absorption onset of the complexes. From the position of HOMO levels and the optical gaps, the LUMO levels of the complexes could be positioned. The calculated data of resulted HOMO and LUMO energy levels are also listed in Table 2.

2.4. Photo- and electroluminescent properties

To optimize the device performance, devices with different doping concentration were studied in the range from 1% to 8% (wt.). Fig. 2 shows the PL spectra of the Ir complexes doped into a blend of PFO–PBD (30%). For comparison, the PL spectrum of the PFO–PBD (30%) film was also included. The PL spectra exhibit two peaks corresponding to the emissions of individual PFO–PBD (30%) and Ir complexes **9**–**11** at low dopant concentrations. With increasing the dopant concentration, the emission originated from host decreases very quickly. Complete quenching of host PL emission occurs at doping concentration of around 8% of Ir complexes. As shown in Table 3, the absolute PL efficiencies of the neat films were 1.7%, 6.3%, and 6.3% for **9**, **10** and **11**, respectively. For comparison, we also listed the PL efficiencies of PBD (100%), PFO (100%) and PFO–PBD (30%) in film. The PL efficiencies of blend films are as high as 40–70%, much higher than those of the complexes in neat films. The high absolute PL efficiency data clearly indicate that no severe host quenching has been observed for all the complexes doped in PFO–PBD (30%) host.

The complexes **9**–**11** were subjected to electroluminescent (EL) characterizations, respectively, with the devices configuration of ITO/PEDOT/PVK/[Ir-complex(*x*%):PFO(30% PBD)]/Ba/Al. The EL spectra are given in Fig. 3. The devices were fabricated with the same blend solutions as used for PL measurement. In EL emission, the emission of PFO–PBD (30%) host was completely quenched at a doping concentration as low as 1%, much lower than that was observed in PL spectra (8%). The fact that complete quenching of host EL emission occurred at a lower doping concentration than that in PL emission implies that the different mechanisms are involved. This points to the fact that the dominant emission mechanism in phosphorescent dye-doped PhLEDs is charge trap-

Table 3
PL efficiencies of PFO–PBD (30%), blends in the solid films (under 325 nm with HeCd laser).

Film composition		PL (%)	Film composition		PL (%)	Film composition		PL (%)
	PBD[a]	51.3		PFO[a]	67.6		PFO–PBD (30%)	86.5
	Ir-100%	1.7		Ir-100%	6.3		Ir-100%	6.3
	Ir-1%	63.7		Ir-1%	72.1		Ir-1%	59.1
9	Ir-2%	59.6	**10**	Ir-2%	47.7	**11**	Ir-2%	54.0
	Ir-4%	78.3		Ir-4%	51.7		Ir-4%	54.8
	Ir-8%	70.4		Ir-8%	62.1		Ir-8%	57.9

[a] Neat film data.

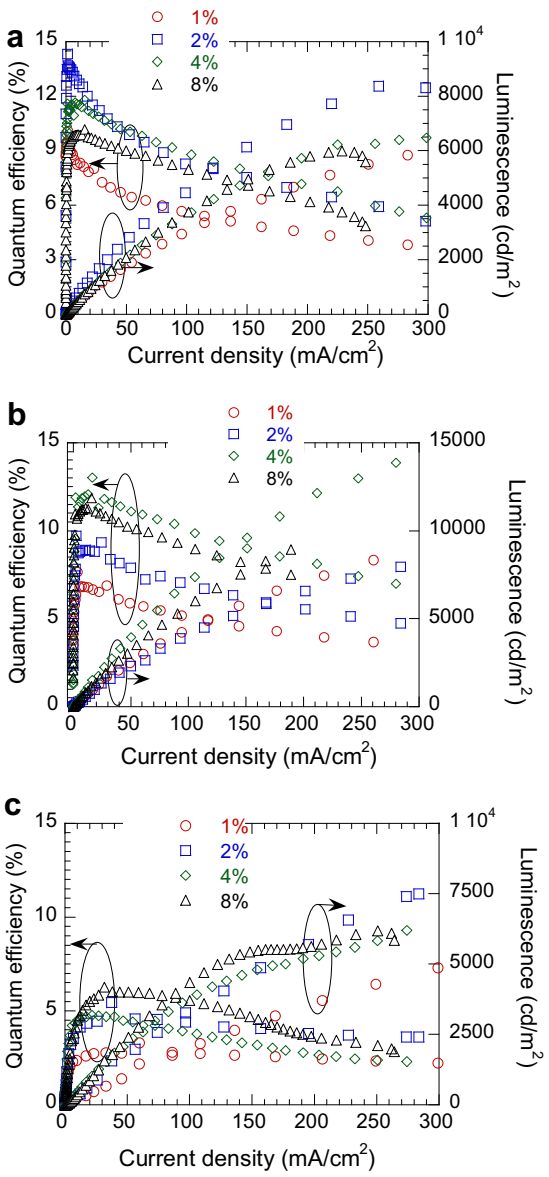

Fig. 4. Quantum efficiency–luminance–current density curves of the devices Ir complexes a (**9**), b (**10**), c (**11**).

ping (rather than Förster energy transfer) followed by carrier recombination on Ir complexes, which has been reported by other authors [31].

Fig. 4 shows external quantum efficiency (EQE) and luminance as a function of current density for devices at different doping concentrations. In the low current region, the efficiency increased with current density because better charge balance was achieved. After reaching the maximum value, EQE went down with current densities, indicating that saturation of dopant emission sites begins to occur. It was reported that PPhLEDs' performance decreases very quickly with the increasing of the dopant concentrations after full energy transfer due to the triplet–triplet annihilation [14]. However, we note that the EQE decay with the increase of current density turned out much gentle for devices from complexes of this study even at high dopant concentrations. For example, for Ir-8% doping concentration devices, good performance were remained at a current density of 100 mA/cm^2 (8.0%, 3757 cd/m^2 for **9**, 9.0%, 6004 cd/m^2 for **10**, 5.6%, 4343 cd/m^2 for **11**, respectively). We attributed this observation to the introduction of 9,9-dimethylfluorenyl that might act as an efficient solubilizing and hindered group to improve the compatibility with the host and prevent significant phosphorescent quenching at mild doping concentrations. It suggested that fluorenyl-substituent attached to 1-phenylisoquinoline remarkably improved the guest-host interaction and prevent triplet–triplet annihilation. We note also that the best doping concentration for maximum device performance varies with different ancillary ligands, viz. 2–4% for **9**, 4–8% for **10** and 8% for **11**. The device characteristics from the Ir complexes were summarized in Table 4. A device with 2% of **9** in PFO–PBD (30%) blend achieved a maximum external quantum efficiency of η_{ext} = 14.3% ph/el and luminous efficiency of LE = 7.8 cd/A with luminous intensity of 95.5 cd/m^2 at a current density of 1.2 mA/cm^2. The CIE coordinates are in the range of saturated red (0.67, 0.32). Device performance slightly decreased with increasing current density and remains as high as 8.3% and 4.5 cd/A at a current density of 100 mA/cm^2. The maximum brightness reached 10 006 cd/cm^2 at a turn-on voltage of 13.5 V and a current density of 412 mA/cm^2. The device with 4% of **10** as dopant shows comparable performance. A η_{ext} = 13.0% ph/el and luminous efficiency of LE = 9.2 cd/A with luminous intensity of 1532 cd/m^2 at a current density of 17 mA/cm^2. The CIE coordinates are also in the range of saturated red (CIE: 0.64, 0.34). The high efficiencies of 9.9% and 7.0 cd/A are remained at 106 mA/cm^2.

In addition, we note that high external quantum efficiencies greater than 10% can be achieved at doping concentrations up to 4–8%. For instance, the external efficiency remained 10.2%, 11.3% and 6.3% when the doping ratio is 8% respectively for **9**, **10** and **11**, which is much higher than that with non-modified 1-phenylisoquinoline as cyclometalated ligand [14,32]. This indicates that modification of the ligands of phosphorescent complexes could inhibit the concentration quenching at the high current density and high concentration due to the complex aggregation.

Table 4
Device performances of iridium complexes **9–11** doped into PFO + PBD (30%).

Complexes	Concentration (%)	V (v)	J (mA/cm^2)	L (cd/m^2)	QE (%)	LE (cd/A)	λ_{max} (nm)	CIE (x, y)
Pqlr	2	15.2	13.7	713	12	5.2	624	(0.67, 0.33)
		19.1	100	4322	9.7	4.2		
9	2	7.0	1.2	95.5	14.3	7.8	636	(0.67, 0.32)
		11.5	100	4464	8.3	4.5		
		13.5	412	10006	4.4	2.4		
10	4	11.0	17	1532	13.0	9.2	616	(0.64, 0.34)
		12.8	106	7380	9.9	7.0		
		14.6	360	15085	5.9	4.2		
11	8	17.6	32	1566	6.3	4.9	618	(0.65, 0.34)
		19.2	100	4343	5.6	4.3		
		22.8	251	6172	3.2	2.5		

3. Conclusion

A new functionalized 1-phenylisoquinoline cyclometallated ligand 1-(3-(9,9-dimethyl-fluoren-2-yl)phenyl)isoquinoline (DMFPQ) for high-efficiency red emitting iridium complexes was synthesized. The phosphorescent polymer light-emitting diodes with the synthesized Ir complexes as dopant emitters and PFO–PBD (30%) blend as the host showed highly attractive external device efficiencies and could compare to that of multiplayer devices with small molecular hosts.

4. Experimental

4.1. Measurements

^{1}H NMR spectra were recorded on a Bruker DRX 300 or 400 spectrometer in deuterated chloroform ($CDCl_3$) solution. The molecular weight of the intermediates and ligands was determined by using a Finnigan Trace GC–MS 2000 Series system. ESI-MS was recorded on a LCQ DECA XP Liquid Chromatography–mass Spectrometry (Thremo Group). Elemental analyses were performed on a Vario EL Elemental analysis instrument (Elementar Co.) UV–Vis absorption spectra were recorded on a HP 8453 spectrophotometer. PL spectra of the complexes in thin film on quartz substrate were recorded on an Instaspec IV CCD spectrophotometer (Oriel Co.) under 325 nm excitation of a HeCd laser. Cyclic voltammetry (CV) was carried out on a CHI660A electrochemical workstation.

4.2. Device fabrication and characterization

The molecular structures of the compounds involved in this device study are shown in Scheme 2. The device structure is ITO/PEDOT (40 nm)/PVK (40 nm)/blend (70 nm)/Ba (4 nm)/Al. The device fabrication followed a standard procedure. The device fabrication was carried out in a controlled atmosphere dry-box (Vacuum Atmosphere Co.) in N_2 circulation. A 40 nm-thick layer of poly(ethylendioxythiophene):poly(styrenesulfonic acid) (PEDOT:PSS), Baytron P 4083, Bayer AG) was spin-cast onto pre-cleaned ITO-glass substrates. After the PEDOT–PSS film dried at 80 °C for 2 h by vacuum, a 40 nm-thick layer of PVK was spin-cast on the top of PEDOT. A mixture of the Ir complexes with [PFO–PBD (30%)] was spin-coated from xylene solution. Typical thickness of emitting layer was 70–80 nm. A thin layer of Ba (4 nm) with Al (130 nm) capping layer was deposited through a shadow mask at a chamber with a base pressure of 3×10^{-4} Pa.

PL spectra and EL spectra were recorded using CCD spectrophotometer (Instaspec 4, Oriel).Profilometer (Tencor Alfa-Step 500) was used to determine the thickness of the films. Ba. Layer thickness was monitored upon deposition by using a crystal thickness monitor (Sycon). Current density(J)–voltage(V)–luminance(L) data were collected using a Keithley 236 source measurement unit and a calibrated silicon photodiode. Absolute PL efficiencies were measured in integrating sphere (IS-080, Labsphere) under 325 nm line of HeCd laser. External EL quantum efficiencies were obtained by measuring a total light output in all directions in an integrating sphere (IS-080, Labsphere). The luminance (cd/m^2) and luminous efficiency (cd/A) were measured by silicon photodiode and calibrated by using a PR-705 Spectra Scan Spectrophotometer (Photo Research).

4.3. Reagents

PFO was supplied by American Dye Sources Inc. PBD was purchased from Aldrich. All manipulations involving air-sensitive reagents were performed in an atmosphere of dry argon. All reagents, unless otherwise specified, were obtained from Aldrich,

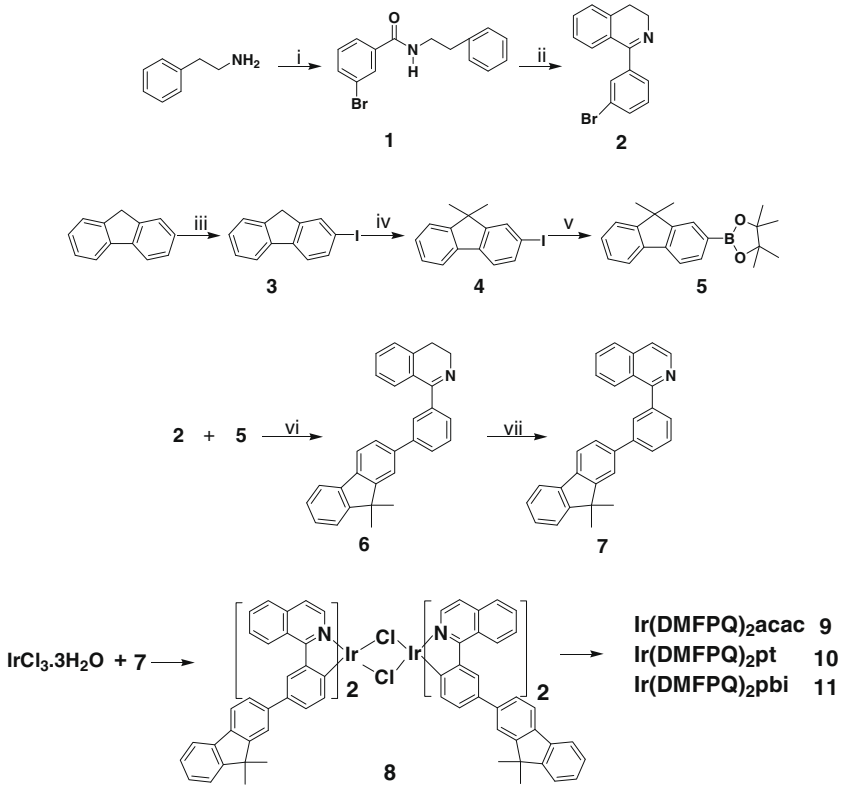

Scheme 1. Synthetic route for the iridium complexes. Reagents and conditions: (v) THF, *n*-BuLi, −78 °C, 2-isopropoxy-4,4,5,5-tetramethyl-1,3,2-dioxaborolane, then to RT, 24 h; (vi) $Pd(PPh_3)_4$, Na_2CO_3, toluene:ethanol = 2:1, 100 °C, Ar, 24 h; (vii) 10% Pd/C, mesitylene, 190 °C, Ar, refluxed 3 h.

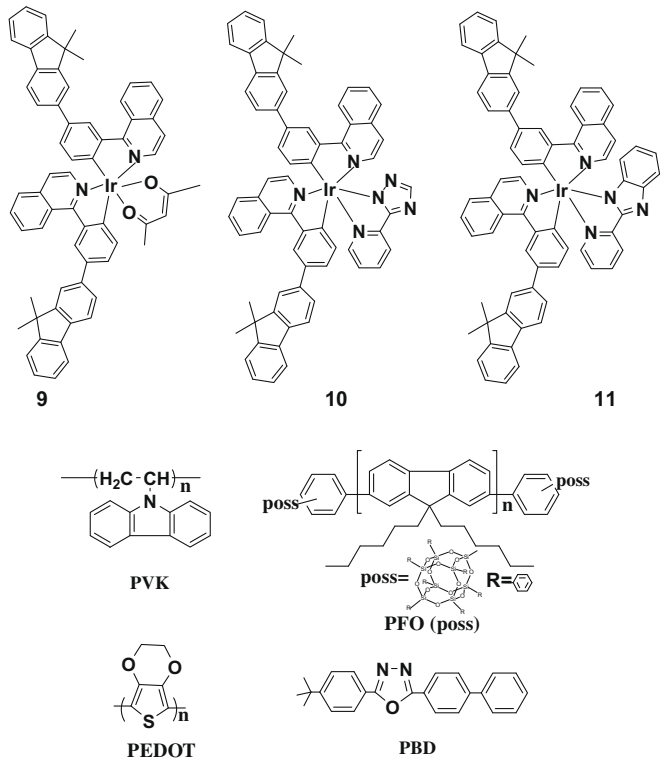

Scheme 2. Molecular structures used for device fabrication.

Acros, and TCI Co. and were used as they were received. THF was distilled over sodium/benzophenone prior to use. Xylene was treated with sodium and distilled. CH_2Cl_2 was dried with anhydrous calcium chloride and distilled. Compounds **1**–**4** were synthesized as reference reported [33]. Syntheses of ligand **7** and Ir complexes **9–11** are shown in Scheme 1.

*2-(4,4,5,5-tetramethyl-1′,3′,2′-dioxaborolan-2′-yl)-9,9-dimethyl-fluorene(**5**).* To a solution of **4** (8.0 g, 0.025 mol) in THF (100 ml) at −78 °C, 15 ml of 1.6 M butyllithium solution in hexane was added dropwise. The mixture was stirred at −78 °C in an atmosphere of dry argon for 2 h. 2-Isopropoxy-4,4,5,5-tetramethyl-1,3,2-dioxaborolane (15 ml) was injected rapidly to the solution. The mixture was stirred at −78 °C for 2 h, then warmed to room temperature and stirred for 24 h. The mixture was poured into water and extracted with ether. The organic layer was washed with brine and dried over anhydrous magnesium sulfate. The solvent was removed under reduced pressure, then purified by column chromatography (silica gel, 10% ethyl acetate in hexane) to give a white powder (4.1 g, 64%). GC–MS: *m*/*z* 320.2(M^+) [34]. ^{1}H NMR($CDCl_3$, 400 MHz) δ($CDCl_3$): 7.90(1H, s), 7.85–7.83(1H, d), 7.78–7.43(2H, m), 7.48–7.44(1H, d), 7.37–7.32(2H, m), 1.52(6H, s), 1.39(12H, s).

*1-(3-(9,9-Dimethyl-fluoren-2-yl)phenyl)-3,4-dihydroisoquinoline (**6**).* A mixture of **2** (1.69 g, 5.91 mmol), **5** (1.89 g, 5.91 mmol), aqueous carbonate sodium (2.95 ml, 2 mol/L), 20 ml toluene, 10 ml of ethanol, were degassed with Ar for 20 min. 0.137 g $Pd(PPh_3)_4$ were added and then heated to reflux for 24 h under Argon. The mixture was allowed to cool to room temperature, and 10 ml of water and 20 ml of dichloromethane were added. The aqueous layer was extracted with dichloromethane and dried with anhydrous magnesium sulfate. The product was purified by column chromatography over silica gel using ethyl acetate:dichloromethane (1:9) as elute to give a pale yellow power (1.70 g, 68.9%). GC–MS: *m*/*z* 399(M^+), ^{1}H NMR δ($CDCl_3$, 400 MHz), 7.92(1H, s),7.78–7.74(3H, m), 7.70 (1H, d),7.62–7.60(1H, q), 7.56–7.55(1H, m), 7.54–7.52(1H, t), 7.45–7.41(1H, m), 7.42–7.39(1H, d), 7.36–7.34(3H, m), 7.33–7.27(2H, t), 3.93–3.89(2H, t), 2.88–2.84(2H, t), 1.54(6H, s).

*1-(3-(9,9-Dimethyl-fluoren-2-yl)phenyl)isoquinoline(**7**).* Compound **6** (1.62 g, 4.1 mmol) was dissolved in 10 ml mesitylene to give a yellow solution, and 0.086 g of 10% Pd/C was added, then refluxed for 3 h at 190 °C under argon. Filtered and washed the black power with dichloromethane several times. The product was purified by recrystallized from the petroleum ether to give pale yellow solid (1.15 g, 71.3%). GC–MS: *m*/*z* 397(M^+), ^{1}H NMR δ($CDCl_3$, 400 MHz): 8.69–8.68(1H, d), 8.21–8.19(1H, d), 8.02(1H, s), 7.94–7.92(1H, d), 7.84–7.80(2H, t), 7.78–7.76(2H, d), 7.77–7.65(5H, m), 7.59–7.56(1H, t), 7.48–7.46(1H, d), 7.34–7.33(2H, m), 1.55(6H, s).

*Tetrakis(1-(3-(9,9-dimethyl-fluoren-2-yl)phenyl)isoquinoline-C2,N′) (μ-chloro-bridged)diiridium(III) **[Ir(dmfpq)$_2$Cl]$_2$** (**8**).* Iridium trichloride hydrate (0.325 g, 0.92 mmol) and **7** (0.915 g, 2.3 mmol) was dissolved in a mixture of 20 ml of 2-ethoxyethanol and water (3:1), and refluxed for 24 h in an argon atmosphere. The solution was cooled to room temperature, and the deep red precipitate was collected on a glass filter frit. The precipitate was washed with 95% ethanol (10 ml) and ethyl ether(10 ml) to give (0.832 g, 88.5%), which was used directly for the next step without purification.

*Bis(1-(3-(9,9-dimethyl-fluoren-2-yl)phenyl)isoquinoline-C2,N′)iridium(III)(acetylacetonate) **[Ir(DMFPQ)$_2$acac]** (**9**).* **8** (0.410 g, 0.20 mmol) was mixed with acetylacetone (0.200 g, 2.0 mmol) and sodium carbonate (0.212 g, 2.0 mmol) in degassed 2-ethoxyethanol (15 ml) in a three-neck flask. The mixture was refluxed in an argon atmosphere for 20 h. After cooling down to room temperature, the dark red precipitate was filtered and washed with water and ethanol. It was purified by column chromatography (silica gel, dichloromethane:petroleum ether = 1:1) to get a deep red powder (0.281 g, 65.0%). ESI-MS: *m*/*z* 985.2(M−100)$^+$, ^{1}H NMR δ($CDCl_3$, 400 MHz): 9.15–9.12(m, 2H), 8.57–8.55 (d, 2H), 8.51(s, 2H), 8.02–7.99(dd, 2H), 7.78–7.72(m, 8H), 7.58–7.54(t, 6H), 7.45–7.42(d, 2H), 7.37–7.31(d, 2H), 7.04–7.01(d, 2H), 6.57–6.55(d, 2H), 5.28(s, 1H), 1.81(s, 6H), 1.50(s, 12H). Anal. Calc. for $C_{65}H_{51}IrN_2O_2$: C, 72.00, H, 4.74; N, 2.58. Found: C, 72.24, H, 4.59, N, 2.18%.

*Bis(1-(3-(9,9-dimethyl-fluoren-2-yl)phenyl)isoquinoline-2,N′)iridium(III)(3-(pyridin-2′-yl)-1,2,4-triazolate) **[Ir(DMFPQ)$_2$pt]** (**10**).* The solution of **pt** [32] (0.186 g, 1.27 mmol) and sodium methoxide (0.082 g,1.5 mmol) in anhydrous ethanol was heated to 50 °C for 1 h. A mixture of **8** (0.305 g, 0.15 mmol) in 2 ml of dichloromethane was dropped to the reaction solution. Then the reaction was refluxed for 3 h and cooled to room temperature. To this were added 50 ml water and 30 ml of dichloromethane. The organic phase was washed with water and dried with anhydrous magnesium sulfate. Further purification by silica-gel column using acetone/dichloromethane (1:1) as an eluent gave a red power (0.162 g, 52.6%). ESI-MS: *m*/*z* 1131.1(M+1)$^+$, ^{1}HNMR δ($CDCl_3$, 300 MHz): d 9.12–9.05(m, 2H), 8.75–8.73(d, 1H), 8.57–8.54(d, 2H), 8.40–8.37(d, 1H), 8.25–8.22(d, 2H), 8.13(s, 1H), 7.94–7.87(m, 4H), 7.84–7.72(t, 7H), 7.66–7.52(d, 4H), 7.45–7.42(m, 4H), 7.38–7.30(m, 4H), 7.29–7.26(t, 1H), 7.18–7.11(m, 2H) 6.62–6.54(q, 2H), 1.54–1.48(dd, 12H). Anal. Calc. for $C_{67}H_{49}IrN_6$: C, 71.19, H, 4.37, N, 7.43. Found: C, 71.33, H, 4.28, N, 7.27%.

*Bis(1-(3-(9,9-dimethyl-fluoren-2-yl)phenyl)isoquinoline-2,N′)iridium(III)(2-(2-pyridyl)benzimidazolate) **[Ir(DMFPQ)$_2$pbi]** (**11**).* The solution of 2-(2-pyridyl)benzimidazole (0.195 g, 1.4 mmol) and sodium methoxide (0.060 g, 1.1 mmol) in anhydrous ethanol was heated to reflux for 1 h. A solution of **8** (0.218 g, 0.11 mmol) in 2 ml of dichloromethane was dropped to the reaction solution. Then the reaction was refluxed for 3 h and cooled to room temperature. Water (50 ml) and 30 ml of dichloromethane were added. The organic phase was washed with water and dried with anhydrous magnesium sulfate. Further purification by silica-gel column using acetone/dichloromethane (1:1) as an eluent gave a red power (0.105 g, 45.2%). ESI-MS: *m*/*z* 1180.2(M+1)$^+$, ^{1}H NMR

$\delta(CDCl_3$, 300 MHz): d 9.11–9.03(m, 2H), 8.61–8.58 (d, 2H), 7.90–7.71(m, 14H), 7.69–7.65(t, 4H), 7.62–7.60(d, 2H), 7.48–7.45(d, 2H), 7.38–7.33(m, 4H), 7.26–7.22(m, 4H), 7.13–7.07(m, 2H) 6.75–6.74(t, 1H), 6.66–6.59(q, 2H), 6.08–6.05(d, 1H), 1.55(s, 12H). Anal. Calc. for $C_{72}H_{52}IrN_5$: C, 73.32, H, 4.44, N, 5.94, Found: C, 73.45, H, 4.27, N, 5.79%.

Acknowledgements

The authors are grateful to the National Natural Science Foundation of China (Nos. 50803008, 50433030, U0634003) and the MOST National Research Project (No. 2009CB623602) for their financial support.

References

[1] E. Holder, B.M.W. Langeveld, U.S. Schubert, Adv. Mater. 17 (2005) 1109.
[2] Y. Ma, H. Zhang, J. Shen, C. Che, Synth. Met. 94 (1998) 245–248.
[3] C.H. Chien, S.F. Liao, C.H. Wu, C.F. Shu, S.Y. Chang, Y. Chi, P.T. Chou, C.H. Lai, Adv. Funct. Mater. 18 (2008) 1430.
[4] M.A. Baldo, S. Lamansky, P.E. Burrows, M.E. Thompson, S.R. Forrest, Appl. Phys. Lett. 75 (1999) 4.
[5] Y.R. Sun, N.C. Giebink, H. Kanno, B.W. Ma, M.E. Thompson, S.R. Forrest, Nature 440 (2006) 908.
[6] Q. Hou, Y. Zhang, F.Y. Li, J.B. Peng, Y. Cao, Organometallics 24 (2005) 4509–4518.
[7] W.G. Zhu, Y.Q. Mo, M. Yuan, W. Yang, Y. Cao, Appl. Phys. Lett. 80 (2002) 2045.
[8] B.H. Tong, Q.B. Mei, S.J. Wang, Y. Fang, Y.Z. Meng, B. Wang, J. Mater. Chem. 18 (2008) 1636.
[9] X.M. Yu, G.J. Zhou, C.S. Lam, W.Y. Wong, X.L. Zhu, J.X. Sun, M. Wong, H.S. Kwok, J. Organomet. Chem. 693 (2008) 1518.
[10] C. Adachi, M.A. Baldo, M.E. Thompson, S.R. Forrest, J. Appl. Phys. 90 (2001) 5048.
[11] Z.L. Wu, Y. Xiong, J.H. Zou, L. Wang, J.C. Liu, Q.L. Chen, W. Yang, J.B. Peng, Y. Cao, Adv. Mater. 20 (2008) 2359.
[12] X.J. Zhang, C.Y. Jiang, Y.Q. Mo, Y.H. Xu, H.H. Shi, Y. Cao, Appl. Phys. Lett. 88 (2006) 051116.
[13] X. Gong, J.C. Ostrowski, G.C. Bazan, D. Moses, A.J. Heeger, Appl. Phys. Lett. 81 (2002) 3711.
[14] C.Y. Jiang, W. Yang, J.B. Peng, S. Xiao, Y. Cao, Adv. Mater. 16 (2004) 537.
[15] Y.M. You, S.Y. Park, J. Am. Chem. Soc. 127 (2005) 12438.
[16] J.C. Ostrowski, M.R. Robinson, A.J. Heeger, G.C. Bazan, Chem. Commun. (2002) 784.
[17] C. Huang, C.-G. Zhen, S.P. Su, Z.-K. Chen, X. Liu, D.-C. Zou, Y.-R. Shi, K.P. Loh, J. Organomet. Chem. 694 (2009) 1317.
[18] P. Coppo, E.A. Plummer, L. De Cola, Chem. Commun. (2004) 1774.
[19] S.C. Lo, R.N. Bera, R.E. Harding, P.L. Burn, I.D.W. Samuel, Adv. Funct. Mater. 18 (2008) 3080.
[20] W.S. Huang, J.T. Lin, C.H. Chien, Y.T. Tao, S.S. Sun, Y.S. Wen, Chem. Mater. 16 (2004) 2480.
[21] J.Q. Ding, J. Gao, Y.X. Cheng, Z.Y. Xie, L.X. Wang, D.G. Ma, X.B. Jing, F.S. Wang, Adv. Funct. Mater. 16 (2006) 575.
[22] A. Tsuboyama, H. Iwawaki, M. Furugori, T. Mukaide, J. Kamatani, S. Igawa, T. Moriyama, S. Miura, T. Takiguchi, S. Okada, M. Hoshino, K. Ueno, J. Am. Chem. Soc. 125 (2003) 12971–12979.
[23] J.P. Duan, P.P. Sun, C.H. Cheng, Adv. Mater. 15 (2003) 224.
[24] C.-H. Yang, C.-C. Tai, I.-W. Sun, J. Mater. Chem. 14 (2004) 947.
[25] L. Wang, B. Liang, F. Huang, J.B. Peng, Y. Cao, Appl. Phys. Lett. 89 (2006) 151115.
[26] Y.H. Xu, B. Liang, J.B. Peng, Q.L. Nlu, W.B. Huang, J. Wang, Org. Electron. 8 (2007) 535.
[27] F.M. Hwang, H.Y. Chen, P.S. Chen, C.S. Liu, Y. Chi, C.F. Shu, F.L. Wu, P.T. Chou, S.M. Peng, G.H. Lee, Inorg. Chem. 44 (2005) 1344.
[28] X. Gong, J.C. Ostrowski, G.C. Bazan, D. Moses, A.J. Heeger, M.S. Liu, A.K.Y. Jen, Adv. Mater. 15 (2003) 45.
[29] A.B. Tamayo, B.D. Alleyne, P.I. Djurovich, S. Lamansky, I. Tsyba, N.N. Ho, R. Bau, M.E. Thompson, J. Am. Chem. Soc. 125 (2003) 7377.
[30] S. Janietza, D.D.C. Bradley, M. Grell, C. Giebeler, Appl. Phys. Lett. 73 (1998) 2453.
[31] P.A. Lane, L.C. Palilis, D.F. O'Brien, C. Giebeler, A.J. Cadby, D.G. Lidzey, A.J. Campbell, W. Blau, D.D.C. Bradley, Phys. Rev. B 63 (2001) 235206.
[32] B. Liang, C.Y. Jiang, Z. Chen, X.J. Zhang, H.H. Shi, Y. Cao, J. Mater. Chem. 16 (2006) 1281.
[33] K. Okumoto, Y. Shirota, Chem. Mater. 15 (2003) 699.
[34] M. Sudhakar, P.I. Djurovich, T.E. Hogen-Esch, M.E. Thompson, J. Am. Chem. Soc. 125 (2003) 7796.